Modeling Sailing Yachts' Course Instabilities Considering Sail Shape Deformations

Emmanouil Angelou, *National Technical University of Athens,* angeloum@mail.ntua.gr

Kostas J. Spyrou, *National Technical University of Athens,* k.spyrou@central.ntua.gr

ABSTRACT

The performance of sailing yachts depends partly on the fluctuating pressure field around the sails which causes continual change of the shape of the sails. The present study focuses on the development of a mathematical model for predicting the behaviour of sailing yachts, with a twofold purpose: to evaluate the variations of forces and moments sustained by the sails due to wind induced sails-shape deformations; and to assess the impact of these variations on the development of course-keeping instability phenomena during downwind sailing conditions. The fluid-structure interaction problem of the sails is handled by coupling, in an iterative way, a Vorticity-Stream Function formulation to a Finite Element Method for flexure elements.

Keywords: *Sailing Yachts, Sail Modeling, Downwind Course*

1. INTRODUCTION

The course stability of sailing yachts is a topic that has not attracted much attention, although, historically, several records exist referring to broaching-to incidents of ships with sails (Spyrou 2010). The present study is a first step towards setting up a systematic study of the course stability of sailing yachts operating in wind and waves. A mathematical model is under development, consisted of two major components: an aerodynamic one, addressing the forces on the sails and the variation of their shape due to wind flow; and a hydrodynamic, handling the hull and its appendages.

Sails produce the aerodynamic forces exploited for propulsion. However, because they are very thin, they have their shape continually adapted according to the locally developing pressures. Thus the flying shape of a sail in real sailing conditions differs from its design shape and it is basically unknown. In terms of physical modelling, one can distinguish sailing cases as *upwind* (running to the wind) where the flow is characterized as lifting and can be assumed as attached to the sails; and as *downwind* (running away from the wind) where viscous effects cannot be disregarded and drag effects are dominant. Recently, the fluid-structure interaction problem of the sails in the upwind case has been tackled, by coupling a low order Boundary Element Method for the aerodynamic part (Lifting Surface) to a Finite Element Method for the structural part (Shell Elements), in combination with an iterative scheme that provided the converged flying shape of the sail and the sustained forces and moments (Angelou & Spyrou 2013).

In the current paper, the sails model is expanded to a wider operational range of inflow angles, from the outskirts of upwind sailing, to beam and fully downwind cases. The method is a pseudo-3d approach, based on the evaluation of vorticity of the flow field around certain cross sections of the sails in order to obtain the force and moment coefficients, while the deformed shape of each sail is obtained using a finite element formulation for flexure

elements. The hydrodynamic part is not complete yet. However, in order to qualitatively evaluate our aerodynamic model we coupled it with a typical semi-empirical manoeuvring model accounting qualitatively for hull reaction and wave forces.

2. MATHEMATICAL MODEL

2.1 Equations of Motion and Coordinate Systems

Since downwind following seas are the cases of main interest, the model includes 4 degrees of freedom, surge, sway, roll and yaw and it used three different coordinate systems: an earth-fixed non-rotating coordinate system (X_0,Y_0,Z_0), a wave fixed body system that travels with the wave celerity (x_w,y_w,z_w) and a body fixed system (x,y,z) with its origin fixed on the midship point where the centerplane and waterplane intersect (Fig. 1);

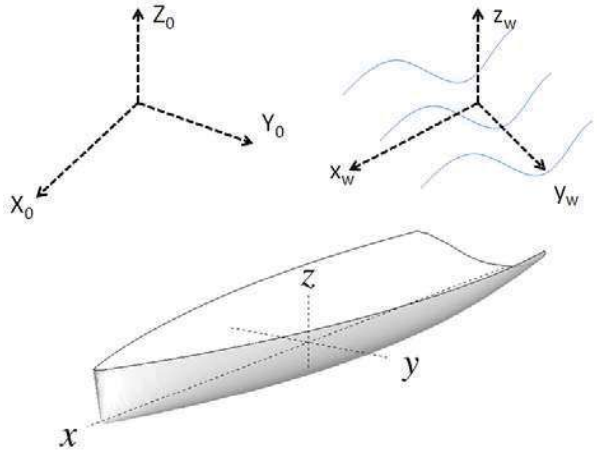

Figure 1: Coordinate Systems.

The systems are in accordance with the right hand rule where 'x' axis points positive forward, having on its left the positive 'y' axis, while positive 'z' axis points upwards.

Assuming the hull as a rigid body, the equations of motions for the 4 degrees of freedom are as in Masuyama & Fukasawa (2011)

$$\left(m+m_x\right)\ddot{x}-\left(m+m_y\cos^2\varphi+m_z\sin^2\varphi\right)\dot{y}\cdot\dot{\psi}= X_{\mathrm{HR}}+X_{\mathrm{R}}+X_{\mathrm{W}}+X_{\mathrm{S}} \tag{1}$$

$$\left(m+m_y\cos^2\varphi+m_z\sin^2\varphi\right)\ddot{y}+ \left(m+m_x\right)\dot{x}\cdot\dot{\psi}+2\left(m_z-m_y\right)\sin\varphi\cos\varphi\cdot\dot{y}\cdot\dot{\varphi}= Y_{\mathrm{HR}}+Y_{\mathrm{R}}+Y_{\mathrm{W}}+Y_{\mathrm{S}} \tag{2}$$

$$\left(I_{xx}+J_{xx}\right)\ddot{\varphi}- \left[\left(I_{yy}+J_{yy}\right)-\left(I_{zz}+J_{zz}\right)\right]\sin\varphi\cos\varphi\cdot\dot{\psi}^2= K_{\mathrm{HR}}+K_{\mathrm{R}}+K_{\mathrm{W}}+K_{\mathrm{S}} \tag{3}$$

$$\left[\left(I_{yy}+J_{yy}\right)\sin^2\varphi+\left(I_{zz}+J_{zz}\right)\cos^2\varphi\right]\ddot{\psi}+ 2\left[\left(I_{yy}+J_{yy}\right)-\left(I_{zz}+J_{zz}\right)\right]\sin\varphi\cos\varphi\cdot\dot{\psi}\cdot\dot{\varphi}= N_{\mathrm{HR}}+N_{\mathrm{R}}+N_{\mathrm{W}}+N_{\mathrm{S}} \tag{4}$$

The subscripts on the right-hand-side of the equations indicate force contribution from *Hull Reaction*, *Rudder*, *Waves* and *Sails*. These terms are grouped into two modules, named *Hull* and *Sails Model* respectively, in accordance with the excitation being of hydrodynamic or aerodynamic origin.

3. SAILS MODEL

3.1 Sails Variation

Sails are surfaces of very small thickness and while this allows a major simplification in the fluid modelling, it simultaneously induces a drawback. This insignificant thickness makes the sail to be a very flexible surface, subjected to deformations due to the pressure forces it sustains under wind flow. Calculating the flow around them then is not enough, as one should

be able to account for the difference between the design shape of the sail and the flying shape it adopts. Moreover, it is important to know the effect this bears to the forces and moments on the sail. Excluding wind tunnel tests and real-time measurements at sea, a common computational approach is to combine a fluid solver for the flow field around the sail with a structural solver for the transition of the initial to the new shape.

Regarding the *upwind* case and in terms of the aforementioned simplification, the small thickness of the sail makes it ideal for being modelled with a potential flow method, such as the one using the Lifting Surface Theory (L.S.T.) (Angelou & Spyrou 2013). This is a formulation for lifting flows that allows the effects of camber and thickness to be decoupled and it is usually applied through a numerical scheme based on the Vortex Lattice Method (V.L.M.). While the lifting surface bears minimal computational cost, it requires that the flow always remains attached to the surface, thus restraining L.S.T.'s applicability to a relatively narrow range of fluid inflow angles.

To examine the behaviour of a sail in a wider operational range, notably *downwind*, as is the scope of this study, the use of viscous flows methods is unavoidable as drag effects become dominant. These methods provide great detail of the flow field, yet they induce a considerable computational cost.

The numerical schemes involving the solution of the Vorticity Transport – Stream Function equations in a computational mesh may appear at first instance outdated compared to modern schemes that handle the primitive variable form of the Navier-Stokes equations. However as the long term objective of this study is directional stability analysis using 6 degrees of freedom while taking into account the instant position and shape of the sail(s), this method was chosen as an intermediate step towards a Lagrangian "free" vorticity formulation, where remeshing of the domain and the induced computational cost can be avoided.

3.2 Sails Modelling

Considering wind flow velocity V_{TW} and a sailing yacht that moves with boat velocity V_B, then the apparent wind, i.e., the wind that actually excites the sails, is defined as in Fossati (2009):

$$V_{AW}^2 = \left(V_{TW} \cdot \cos a_{TW} + V_B\right)^2 + V_{TW} \sin a_{TW} \cos^2 \varphi \tag{5}$$

$$a_{AW} = \operatorname{atan}\left(\frac{V_{TW} \sin a_{TW} \cos \varphi}{V_{TW} \cos a_{TW} + V_B}\right) \tag{6}$$

where a_{TW} is true wind angle and a_{AW} is the apparent wind angle.

The sail forces are obtained in terms of *drag* (C_D) and *lift* (C_L) coefficients, where *drag* (D) is the resulting force on the direction of the free stream flow (apparent wind), while *lift* (L) is normal to it:

$$D = \frac{1}{2} \rho \cdot V_{wind}^2 \cdot S \cdot C_D \tag{7}$$

$$L = \frac{1}{2} \rho \cdot V_{wind}^2 \cdot S \cdot C_L \tag{8}$$

Through transformation to the ship coordinate system the surge and sway forces are obtained:

$$X_S = D \cdot \cos a_{AW} + L \cdot \sin a_{AW} \tag{9}$$

$$Y_S = D \cdot \sin a_{AW} + L \cdot \cos a_{AW} \cdot \cos \varphi \tag{10}$$

Roll and yaw sail induced moments are:

$$K_S = -Y_S \cdot z_{cef} \cdot \cos \varphi \tag{11}$$

$$N_S = \left(Y_S \cdot xcef + X_S \cdot ycef\right) \qquad (12)$$

In this study, the method of aerodynamic force calculation is pseudo-transient, meaning that calculations are performed on certain sections of the sails, and vertical flow interaction effects are ignored. Every section has a computational flow field constructed around it, in the form of an unstructured meshed domain of triangular elements. A Finite Volume numerical scheme is applied on these elements for the solution of the Vorticity Transport and Stream Function equations.

Once the velocity and pressure fields are computed, pressure loads are transformed to nodal forces and they are used for deriving the deformation of the sail via a Finite Element Formulation for flexure beams. When the sail shape has converged, lift and drag coefficients of the section are used in order to calculate total sail excitation. Each section sail coefficient (red lines Fig. 2) is averaged over a surface that extends bilaterally off the section's vertical position (black lines Fig. 2). Total Drag and Lift forces of the sail are defined as

$$D = \frac{1}{2}\rho \cdot V_{wind}^2 \cdot \sum\left\{S_i \cdot C_{Di}\right\} \qquad (13)$$

$$L = \frac{1}{2}\rho \cdot V_{wind}^2 \cdot \sum\left\{S_i \cdot C_{Li}\right\} \qquad (14)$$

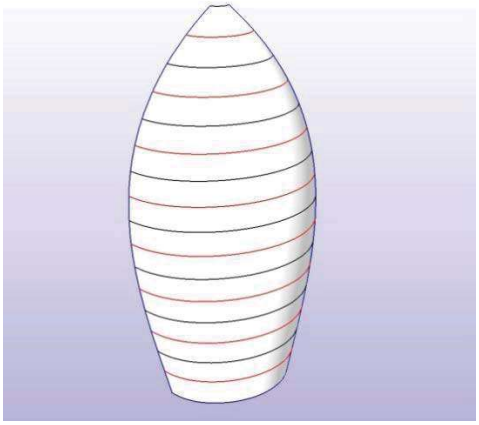

Figure 2: Spinnaker Sail and sections.

3.3 Meshing

The mesh is constructed using the Advancing Front Method – AFV (Peraire et al 1987), which was chosen due to its ability to handle complex geometries whilst its implementation is straightforward. Given the boundary of an outer domain Ω and any internal boundaries Ω_i, this formulation creates an initial front of connected segments, each of which is used as the edge of a candidate triangle element to be added. With every triangle addition, the respective initial segment is replaced by the new edge or edge(s), and the front is reduced until the domain is completely meshed.

However, the obtained mesh may contain triangles with highly acute angles, prone to cause numerical errors during the solution. To overcome this, the smoothing technique of Zhou & Shimada (2000) is applied on the domain. This method treats all triangle edges as springs, either on a compressed or on an elongated state. By iterating through probable nodal positions, this method seeks to find an optimized set, where the torsional energy of every spring is minimized. All non-boundary nodes are moved accordingly and each triangle tends to reach an equilateral shape (Fig. 3).

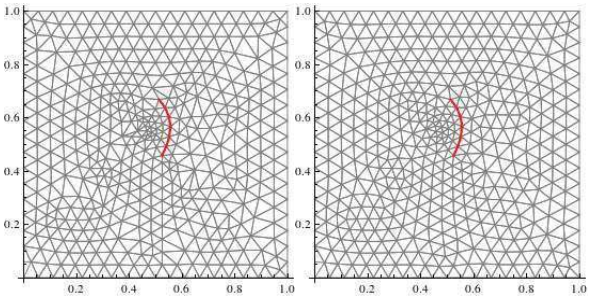

Figure 3: Initial (left) and Smoothed (Right) Mesh around a Sail Section (Bold Red).

While the obtained mesh is smoothed, the size of the triangles in regions away from the given boundaries tends to increase. This is a drawback in accuracy, especially in case the triangles are located in areas where state variables are characterized by large gradients.

A future step is the local refinement in these areas using mesh enrichment techniques.

3.4 Aerodynamic Component

The fluid domain around the sails is obtained by solving the non-conservative Vorticity Transport Equation (15) and the Stream Function Equation (16) using a Finite Volume scheme on an unstructured triangular meshed domain. The triangles are virtually treated as P2 elements, meaning that mid-edge point values of vorticity are included in the calculations, but only in order to update the vorticity on the centres and vertices.

$$\frac{\partial \omega}{\partial t} + u\frac{\partial \omega}{\partial x} + v\frac{\partial \omega}{\partial y} = \nu\left(\frac{\partial^2 \omega}{\partial x^2} + \frac{\partial^2 \omega}{\partial y^2}\right) \quad (15)$$

$$\frac{\partial^2 \psi}{\partial x^2} + \frac{\partial^2 \psi}{\partial y^2} = -\omega \quad (16)$$

The numerical solution of the Vorticity Transport equation is dictated by the viscous split technique where the advection and diffusion terms are treated separately (e.g. see Cottet & Koumoutsakos, 2000) :

$$\frac{\partial \omega}{\partial t} + u\frac{\partial \omega}{\partial x} + v\frac{\partial \omega}{\partial y} = 0 \quad (17)$$

$$\frac{\partial \omega}{\partial t} = \nu\left(\frac{\partial^2 \omega}{\partial x^2} + \frac{\partial^2 \omega}{\partial y^2}\right) \quad (18)$$

The pure advection part (17) of the Vorticity Transport equation is treated using the fluctuation-splitting scheme of Nishikawa & Roe (2005). This method provides a way for the calculation of the fraction of the fluctuation of a variable inside any triangle, as that fluctuation is directed to the triangle's downstream nodes. The nodes are characterized as upwind or downwind, according to the triangle's orientation in relation with the local convection velocity vector $\vec{V}$. Thus, in every triangle, transport effects are accounted for, by updating only the downstream nodes.

The pure diffusion equation (18) is treated as in Hoffman & Chiang (2000). Considering any triangle T, by applying Green's theorem on the surface integral of the diffusion equation, the right hand side is transformed to a line integral that can be calculated using the mid-point vorticity values of the triangle edges. These are obtained by interpolation of vorticity value that is assigned on the neighbouring triangles centres, as also on the common nodes they share with triangle T.

The Stream Function, as in Hoffman & Chiang (2000), can be transformed from an elliptic (16) to a pseudo-transient (19) parabolic equation:

$$\frac{\partial \psi}{\partial t} = -\left(\frac{\partial^2 \psi}{\partial x^2} + \frac{\partial^2 \psi}{\partial y^2} + \omega\right) \quad (19)$$

Equation (19) is treated as the diffusion equation (18) with the addition of the calculated vorticity during the current time step as a source term.

The free stream flow is considered to enter a rectangular computational domain from the left side bearing horizontal velocity of constant magnitude u_0, and exit from the right side far downstream of the sails. The same value of inflow velocity is considered at the top and bottom domain boundaries in order to simulate infinite fluid extent normal to them. The stream function is assigned a constant value across the bottom boundary and gradually increases with increasing height according to $u = \partial\psi/\partial y$ so as to provide a constant velocity u_0. The stream function value on the top boundary remains constant until the end of the domain. Initial vorticity values have been set to zero all over the domain. When the wind vector has a non-zero angle of attack then inflow conditions for the velocity remain the same and it is the initial geometry of the sail that is rotated accordingly.

3.5 Aeroelastic Component

The structural response of every discrete sail section to wind loads is modelled using a Finite Element Method for *flexures*. A flexure is an enriched beam element, capable of being subjected to both axial and bending loading. Each section is divided to small segments that correspond to all triangle edges that consist of sail nodes explicitly. Considering a linearly elastic, isotropic and homogeneous material, the displacements **U** of the nodes are calculated by solving the linear system

$$K_{STIFF} \cdot \boldsymbol{U} = \overrightarrow{\boldsymbol{F}} \tag{20}$$

The total stiffness matrix K_{STIFF} is composed by superposition of all element stiffness matrices k_E according to their connectivity. The matrix k_E is a joint matrix of a bar and a flexure element, for axial and bending loads respectively without considering any coupling between them. The formation of the bending flexure stiffness matrix for each segment is obtained through the application of the first theorem of Castigliano, with respect to nodal translational and rotational displacements, to the strain energy function U_E of the element (Hutton 2004).

$$U_E = \frac{1}{2}\int \sigma_x \varepsilon_x \mathrm{d}V \tag{21}$$

Assuming that each segment can be considered as an elastic bar of constant cross section, the axial stiffness matrix of the element is formulated by analyzing the axial forces using the stress and strain formulae (Hutton 2004). After solving the linear system, nodal positions are adjusted according to the displacements vector of the solution and the domain is re-meshed.

4. HULL MODEL

As the scope of this study is to emphasize on the sail-induced impact on the development of instabilities, the hull modular parts of the mathematical model have been treated so far using methods that do not necessarily lead to a precise quantification of hull responses. In addition, as the appendages have been approximated by simplified geometries and in the general case flow interaction effects between them have been omitted, hull realistic modelling is underacted. However as this manoeuvring model is still under development and bears a potential for growth of modelling detail regarding the modular parts it consists of, compromising with low level analysis on these components has been tolerated.

4.1 Inertia Terms

The calculation of the moments of inertia is based on the mass distribution of the yacht. For the canoe body, the added masses along y and z axes are calculated by considering sections along the hull and approximating their corresponding added mass coefficients from Korotkin (2008), while for the x axis and added moments of inertia around all axes as in Ridder (2004). The appendages are treated as elongated ellipsoids and their added masses as also their added moments of inertia are approximated as in Korotkin (2008).

4.2 Resistance

The resistance of the yacht can be decomposed to viscous, induced (which is the lift-induced Drag force component that is developing on the body and appendages due to the inflow angle) and wave-making parts. Viscous and induced terms are calculated as in Oossanen (1993) with some modifications regarding the contribution of the canoe body of the hull and the bulbous part of the keel, where a drag coefficient and a form factor have been added respectively, as in Nesteruk & Cartwright (2011) and in Scragg & Nelson (1993). Wherever included in the above formulation, the wetted surface is calculated from the summation of the areas of the hull

panels (Fig. 4) that are immersed at that instant under heel, if any. Lastly, the wave-making resistance of the yacht is calculated as in Pascual (2007).

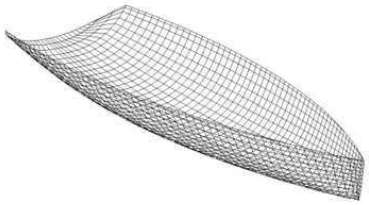

Figure 4: Canoe Body Panels.

4.3 Other Hull Reaction and Rudder

Other hull reaction forces and moments for sway and yaw modes are taken into account using the model of Inoue et al (1979), where the linear hydrodynamic coefficients are as in Clarke (1983) and the nonlinear as in Inoue et al(1979). Heel effects for the same modes have been added as in Hirano & Takashina (1980). Though the aforementioned references provide coefficients suitable for much larger hulls and need treatment regarding appendages effects, they were chosen as a rough indication due to our lack of data regarding the hydrodynamic responses of the studied sailing yacht. Roll terms are limited to damping and restoring moments. Rudder forces and moments in the model are accounted for as in Masuyama&Fukasawa (2011).

4.4 Waves

Considering an undisturbed pressure field around the yacht, the wave excitation is limited to Froude-Krylov forces and moments. These are calculated by integrating the unit potential φ_0 (e.g. Belenky & Sevastianov 2003) on every immersed panel of the hull up to the elevated running waterline, after the panel coordinates have been transformed suitably for the relative position of the hull on the encountered wave.

5. CASE STUDY– RESULTS

5.1 Principal Dimensions

Problems of course stability in strong wind are well known for motorships (e.g. Spyrou 1995, Spyrou et al 2007), while for sailing yachts the available studies are only a few (e.g. Harris et al 2000). The yacht used as a case study is a one-mast modern cruiser, carrying a mail and a jib sail, or a main and a spinnaker sail, for upwind and downwind courses respectively. Principal dimensions of the hull are on table 1.

HULL	
Length Overall	13.90 m
Length Waterline	12.86 m
Beam Waterline	2.79 m
Draught [Canoe Body | Total]	0.525 m | 3.45 m
Displacement	7830 kg

Table 1.Hull and Sails Dimensions.

The concept of the first two "trial" simulated scenarios is to apprehend the sensitivity of the model. The first scenario handles a case where the yacht is sailing under the influence of constant wind of 10 knots speed and $a_{TW}=0^o$ direction off the stern (*true* wind angle) while wave excitation is omitted.

After a small simulated time (t =10sec) the wind direction is considered to change to $a_{TW}=10^o$ off the stern while the rudder angle is kept fixed to zero position. On both cases counter-rotating vortices develop in front and back of the sail (Fig.5). This vorticity trend was expected, as compared with a bluff canopy body, bearing strong similarity to a sail (Johari & Desabrais 2005). As the wind angle changes, the yacht commences a turn. Trajectory and responses for 30 seconds of simulation are depicted in Figures 6 to 8.

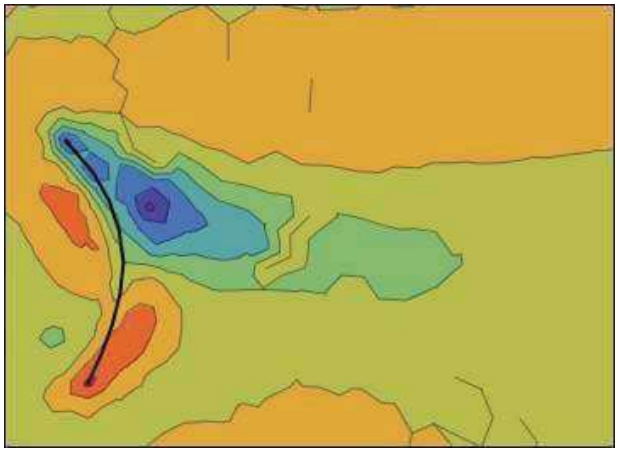

Figure 5a: Vorticity field, V_{wind}: 10kn, a_{TW}: 0°

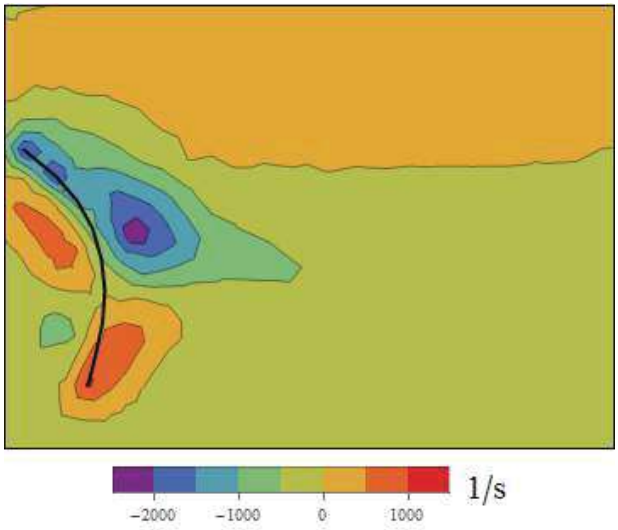

Figure 5b: Vorticity field, V_{wind}: 10kn, a_{TW}: 10°

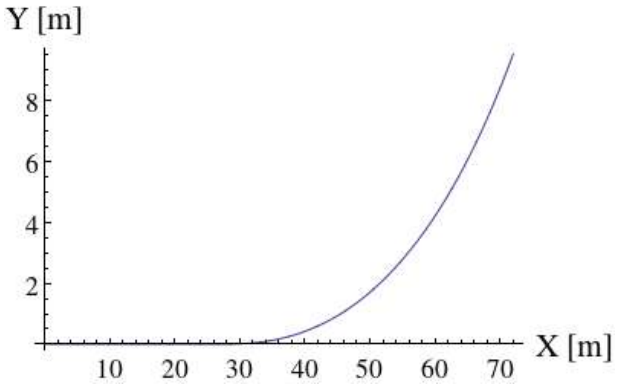

Figure 6: Course trajectory: scenario 1.

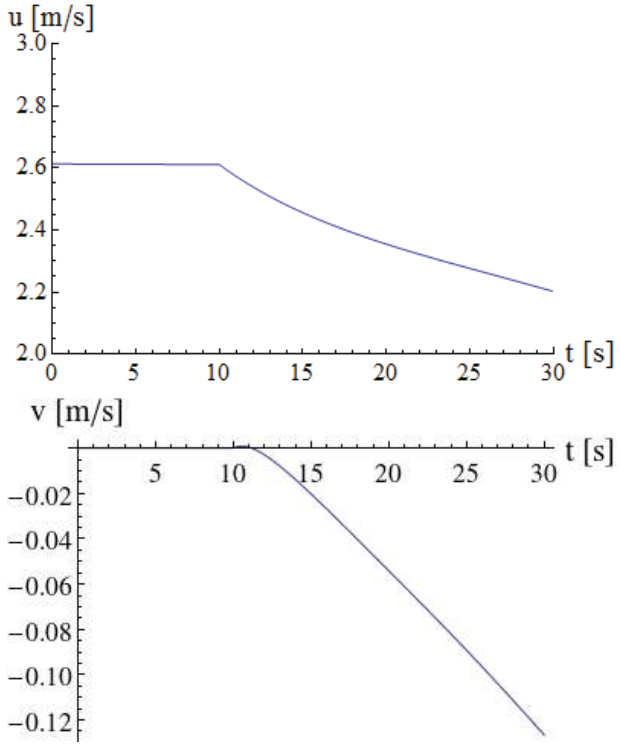

Figure 7: Surge (top) and sway (bottom) velocity.

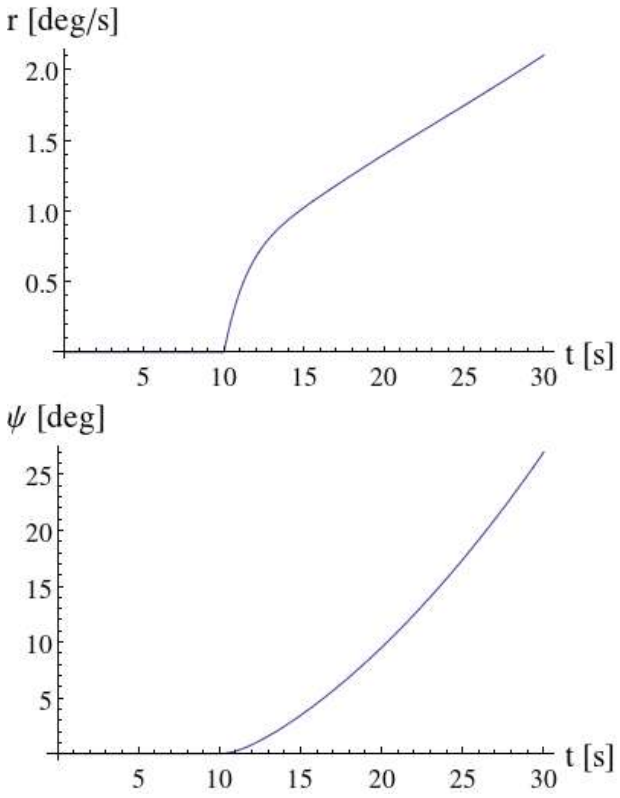

Figure 8: Yaw turning rate (top) and angle (bottom).

In the second scenario the yacht is sailing under the influence of a purely following *true* wind (0^o off the stern) of constant speed of 10 knots. Simultaneously it is excited by following harmonic waves of λ= 1.5 L_{wl} with steepness H/λ=0.036. As shown in Fig. 9, the yacht experiences asymmetric surging. Moreover, for a very steep wave (H/λ=0.051) it adopts surf-riding behaviour (Fig. 9).

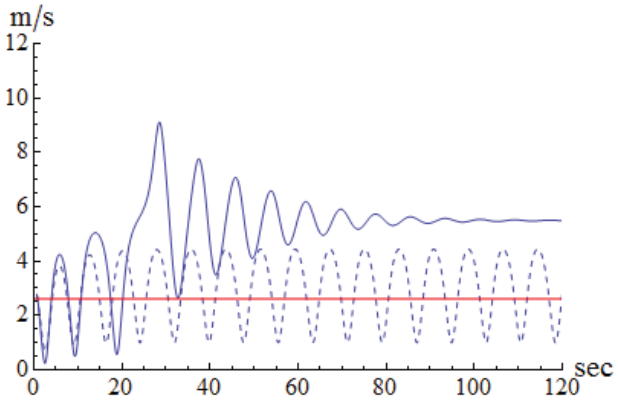

Figure 9: Asymmetric surging and surf-riding.

6. CONCLUSIONS – FUTURE WORK

This study is the first step towards a mathematical model suitable for the analysis of directional instabilities phenomena of sailing yachts. As the authors' intention is to evaluate the impact of sail shape deformations and sail forces variations on the behaviour of yachts, the hull model has been formulated inside the context of low level detail analysis, while the sails have been modelled by coupling two relatively simple models, among the family of the finest advanced methods: a pseudo-3d Vorticity-Stream function formulation and a Finite Element Method for flexure elements.

The performance of the sails model seems realistic, in qualitative terms. Future steps include further development by implementing turbulence effects and by moving towards a full 3d method for both the fluid and structural formulations.

The hull model has proved to be hypersensitive to excitations. This was expected and it is attributed to the choice of handling (in lack of any full scale data or of a more appropriate formulation) the performance of a small sailing yacht using methods intended for hulls of significant greater displacement; doing so, the influence of the appendages was underacted and the damping of the hull underestimated.

The same method used for the fluid part of the sails model can be modified to tackle the problem of finding a realistic pattern of hull reaction forces and moments.

7. ACKNOWLEDMENTS

Mr. Angelou acknowledges with gratitude his support by NTUA's PhD Research Fund for Doctoral Candidates (ΕΛΚΕ).

8. REFERENCES

Angelou, E. and Spyrou, K.J., 2013, "Simulations of Sails of a Yacht Using a Fluid-Structure Interaction Model", 10th HSTAM International Congress on Mechanics, Chania, Greece.

Belenky, V.L. and Sevastianof, N.B., 2003, "Stability and Safety of Ships, Vol. II : Risk of Capsizing", Elsevier Ocean Engineering Book Series, Vol.10-II, pp. 83-86.

Clarke D., Gedling P. and Hine G., 1983, "The Application of Manoeuvring criteria in Hull Design using Linear Theory", RINA Transactions, Vol. 125, pp. 45-68.

Cottet, G.H., Koumoutsakos, P.D., 2000, "Vortex Methods: Theory and Practice", Cambridge University Press, Cambridge, UK.

Fossati, F.,2009, "Aero-Hydrodynamics and the Performance of Sailing Yachts", Adlard Coles Nautical, London, pp. 265-287.

Harris, D., Thomas, G., Renilson, M., 2000, "Towards Predicting the Behaviour of Yachts in Following Seas", 7th International Conference on Stability of Ships and Ocean Vehicles, pp. 595-608.

Hirano, M. and Takashina, J., 1980, "A Calculation of Ship Turning Motion Taking Coupling Effect Due to Heel into Consideration", Journal of the West-Japan Society of Naval Architects and Ocean Engineers, Vol. 59, March 1980, pp. 71-81.

Hoffmann, K.A. and Chiang, S.T., 2000, "Computational Fluid Dynamics", Vol. II, Engineering Education System, pp. 391-402.

Hutton, D.V., 2004, "Fundamentals of Finite Element Analysis", Mc-Graw Hill, pp. 91-131.

Inoue, S., Hirano, M. and Mukai, K., 1979, "The Non-linear Terms of Lateral Force and Moment Acting on Ship Hull in Case of Maneuvering", The Japan Society of Naval Architects and Ocean Engineers, Vol 58, August 1979, pp. 153-160.

Johari, H. and Desabrais, J.K., 2005, "Vortex Shedding in the Near Wake of a Parachute Canopy", Journal of Fluid Mechanics, vol. 536, pp.185-207.

Korotkin, A.I., 2008, "Added Masses of Ships Structures, Springer, Series of Fluid Mechanics and its Applications, Vol.88, pp. 82.

Masuyama, Y. andFukasawa T., 2011, "Tacking Simulation of Sailing Yachts with New Model of Aerodynamic Force Variation During Tacking Maneuver", SNAME Journal of Sailboat Technology, Article 2011-01.

Nesteruk, I. and Cartwright, J.H.E., 2011, "Turbulent Skin-Friction Drag on a Slender Body of Revolution and Gray's Paradox", 13th European Turbulence Conference (ETC13), Journal of Physics: Conference Series 318.

Nishikawa, H. and Roe, L.P., 2005, "Towards High-Order Fluctuation-Splitting Schemes for Navier-Stokes Equations", 17th AIAA CFD Conference, Toronto.

van Oossanen, P., 1993, "Predicting the Speed of Sailing Yachts", SNAME Transactions, Vol. 101, pp. 337-397.

Pascual, E., 2007, "Revised Approached to Khaskind'sMethod to Calculate the Wave-Making Resistance Depending on the Sectional Area Curve of the Ship", Journal of Ship Research, Vol. 51, September 2007, pp. 259-266.

Peraire, J., Vahdati, M., Morgan, K. and Zienkiewicz, O.J., 1987, "Adaptive Remeshing for Compressible Flow Computations", Journal of Computational Physics, Vol. 72, pp. 449-466.

Ridder, E.J., Vermeulen, K.J. and Keuning, J.A., 2004, "A Mathematical Model for the Tacking Maneuver of a Sailing Yacht", The International HISWA Symposium on Yacht Design and Yacht Construction, Amsterdam, Netherlands.

Scragg C.A. and Nelson B.D., 1993, "The Design of an Eight-Oared Rowing Shell", SNAME Marine Technology, Vol. 30, No.2, April 1993, pp. 84-49.

Spyrou K., 1995, "Yaw Stability of Ships in Stationary Wind", Ship Technology Research/Schiffstechnik, 42, No.1, pp. 21-30.

Spyrou K., Tigkas, I., Hatzis, A., 2007, "Dynamics of a Ship Steering in Wind

Revisited", Journal of Ship Research, 51, pp. 160-173.

Spyrou, K.J., 2010, "Historical Trails of Ship Broaching-To", The Transactions of the Royal Institution of Naval Architects: Part A - International Journal of Maritime Engineering, 152, Part A4, pp. 163-173.

Zhou, T. and Shimadi, K., 2000, "An Angle-Based Approach to Two-Dimensional Mesh Smoothing", Proceedings of the Ninth International Meshing Roundtable, New Orleans, pp. 373–384.